

000 RETHINKING GRAPH-BASED DOCUMENT CLASSIFI- 001 CATION: LEARNING DATA-DRIVEN STRUCTURES BE- 002 YOND HEURISTIC APPROACHES 003

004 **Anonymous authors**
 005
 006

007 Paper under double-blind review
 008
 009

010 ABSTRACT 011

012 In document classification, graph-based models effectively capture document
 013 structure and overcome sequence length limitations, enhancing contextual under-
 014 standing. However, existing graph document representations often rely on heuris-
 015 tics, domain-specific rules, or expert knowledge. We propose a novel method to
 016 learn data-driven graph structures, eliminating the need for manual design and
 017 reducing domain dependence. Our approach constructs homogeneous weighted
 018 graphs with sentences as nodes, while edges are learned via a self-attention model
 019 that identifies dependencies between sentence pairs. A statistical filtering strategy
 020 retains only strongly correlated sentences, improving graph quality while reduc-
 021 ing the graph size. Experiments¹ on three datasets show that learned graphs con-
 022 sistently outperform heuristic-based baselines and recent small language models,
 023 achieving higher accuracy and F_1 score. Furthermore, our study demonstrates
 024 the effectiveness of the statistical filtering in improving classification robustness,
 025 highlighting the potential of automatic graph generation over traditional heuristic
 026 approaches and opening new directions for broader applications in NLP.
 027
 028

029 1 INTRODUCTION 030

031 Traditional vector-based text representation methods often struggle to effectively capture the struc-
 032 tural information inherent in text, particularly when dealing with long documents. In contrast, graph-
 033 based representations have emerged as a powerful alternative, enabling the modeling of dependen-
 034 cies between textual units and leveraging their structure to better capture and differentiate local
 035 contexts within a document. Such representations have demonstrated promising results in document
 036 classification tasks (Zhang et al., 2020; Wang et al., 2023; Gu et al., 2023; Li et al., 2025b), with
 037 various graph construction strategies proposed to date.

038 However, existing graph-based approaches heavily rely on domain-specific heuristics and expert
 039 knowledge, limiting their generalizability across tasks. As noted by Wang et al. (2024), graph
 040 structures in text classification are typically implicit and require manual design tailored to each
 041 application. Consequently, these methods are typically effective only within narrow, predefined
 042 scenarios (Bugueño & de Melo, 2023; Galke & Scherp, 2022). To reduce the reliance on manually
 043 defined heuristics, a more robust and adaptive approach is needed.

044 While attention mechanisms have been widely adopted to model long-range dependencies, their
 045 usage to induce latent relational structure remains underexplored in document classification. In
 046 this work, we view attention scores as potential evidence for semantic ties between textual units,
 047 serving as a data-driven proxy for graph topology. Through statistical filtering, we derive sparse,
 048 task-conditioned relational structures that adapt to a document’s internal organization rather than
 049 reflecting externally imposed heuristics.

050 We introduce a self-attention-based framework that, to our knowledge, is the first to automatically
 051 learn graph structures for document representations without handcrafted heuristics (see Figure 1).
 052 Our method builds homogeneous graphs where nodes represent sentences and edges are determined
 053

¹<https://github.com/available/upon/publication>

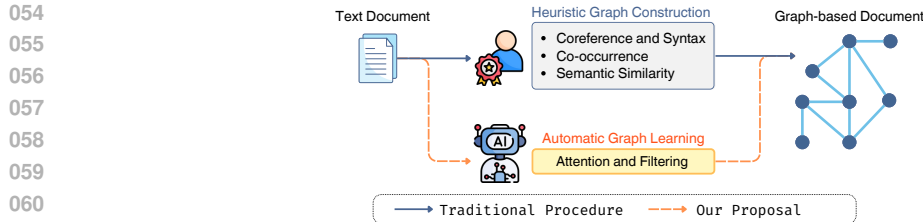


Figure 1: Instead of using domain-specific heuristics for graph construction, we learn graph structures from text, eliminating task-specific design and enhancing generalization.

by an attention model that learns relationships between sentence pairs. A statistical filtering step—using mean- or max-bound thresholds derived from the learned weight distribution—retains only the most salient relationships.

We evaluate our approach on three document classification datasets of varying lengths, comparing our learned graphs to five widely used heuristic-based construction strategies—complete graph, sentence order (Castillo et al., 2015; Bugueño & de Melo, 2023), window-based co-occurrence (Hassan & Banea, 2006; Rousseau et al., 2015; Zhang et al., 2020; Li et al., 2025b), and semantic similarity under predefined thresholds (Li et al., 2025b; Mihalcea & Tarau, 2004; Bugueño et al., 2024)—as well as competitive transformer and embedding-based models (Section 4.2). The results reveal that attention-learned graphs consistently outperform heuristic graphs and recent non-graph baselines, with gains becoming more pronounced as the document length increases. Further analysis finds that max-bound filtering is most effective for long documents, while mean-bound filtering fares better on medium-length documents. These findings highlight the potential of data-driven graph learning over conventional heuristic approaches and open new directions for broader applications.

The key contributions of this paper are:

- A novel data-driven graph generation model: We introduce a self-attention-based approach that learns sentence-level graph structure directly from data, eliminating reliance on heuristic rules or domain-specific design. Unlike prior graph structure learning methods that jointly optimize the graph and its downstream graph classifier, our method operates independently from the graph encoder, enabling flexible and architecture-agnostic graph generation.
- A variance-aware statistical sparsification mechanism: We introduce mean- and max-bound filtering strategies that convert dense and noisy attention patterns into sparse, reliable document graphs by selecting statistically salient inter-sentence dependencies.
- Strong performance gains over heuristic graphs and non-graph baselines: Across datasets, our learned graphs improve accuracy by up to 4 points and macro- F_1 by 4.3 points over heuristic graphs, and by up to 2.7 points over recent small language models.
- Comprehensive evaluation and analysis: We benchmark our approach against five heuristic-based graph construction methods, two transformer baselines, and two embedding-based baselines, and analyze structural properties, resource usage, and the behavior of our filtering strategies on three publicly available datasets.

2 RELATED WORK

2.1 PREDEFINED GRAPH SCHEMES

Classic Approaches. Numerous graph-based text representation approaches have been used in text classification, demonstrating their effectiveness in capturing textual relationships. Early methods primarily relied on co-occurrence statistics and linguistic patterns, often representing words as nodes and connecting them if they co-occur within a fixed-size sliding window (Mihalcea & Tarau, 2004; Hassan & Banea, 2006; Rousseau et al., 2015; Zhang et al., 2020). Sequence-based graphs offer a complementary approach, connecting words based on their original order. While early implementations used weighted edges by frequency (Castillo et al., 2015), recent work suggests that binarized edges can improve performance (Bugueño & de Melo, 2023).

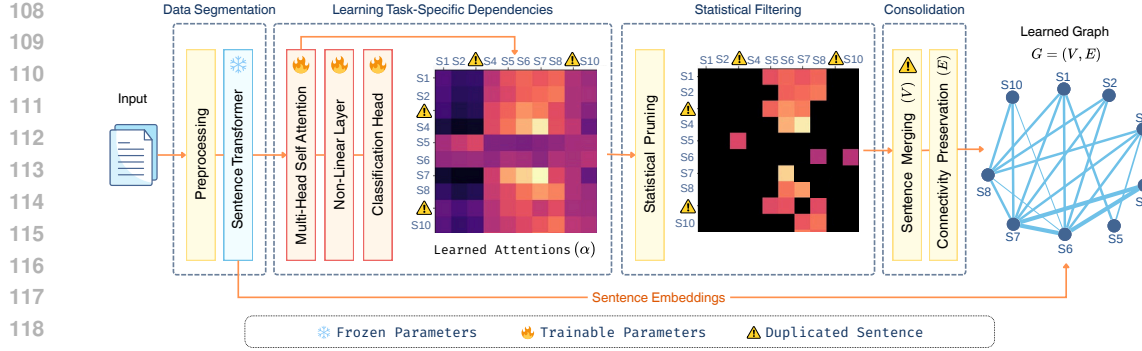


Figure 2: Overview of our framework. Non-trainable steps include *data segmentation*, *statistical filtering*, and *consolidation*, while the Sentence Transformer is used with frozen parameters. Edge widths in graph G reflect learned edge weights, with thicker edges denoting stronger dependencies.

Recent Approaches. More sophisticated methods have been introduced to enhance textual modeling. TextGCN (Yao et al., 2019) builds a global heterogeneous graph with word and document nodes, using Point-wise Mutual Information (PMI) for weighting word–word edges and TF-IDF for word–document links, whereas TextLevelGCN (Huang et al., 2019) generates one graph per document by connecting word nodes (duplicated when repeated) based on co-occurrence within a sliding window, also weighted by PMI.

Extensions enrich graphs with additional heterogeneous elements, such as topic nodes (Gu et al., 2023; Cui et al., 2020), word and character n-grams (Li & Aletras, 2022), label nodes (Li et al., 2024), or document metadata including keywords, entities, and titles (Ai et al., 2023). Other studies incorporate multiple edge types while maintaining a single node type, encoding features such as titles, keywords, or events for document nodes (Ai et al., 2025), or combining co-occurrence, syntactic dependencies, and self-loops for word nodes (Wang et al., 2023). An alternative strategy (Li et al., 2025b) constructs separate graphs for words and sentences that are fused during training.

Limitation. Despite their progress, existing methods share a fundamental limitation: reliance on predefined domain knowledge to establish node and edge types, making them heavily task- and domain-specific. To address this, a learning-based approach for automatic graph structure discovery can offer a more generalizable and adaptable alternative by removing the need for manual design.

2.2 LEARNING THE DOCUMENT STRUCTURE

To the best of our knowledge, no existing method learns document graph structures directly from raw text. Instead, they depend on domain-specific heuristics for graph construction. While some studies incorporate graph-based techniques to enrich contextual representations, they do not explicitly learn the graph topology itself.

The most relevant work (Xu et al., 2021) combines a Graph Attention Network (GAT) (Veličković et al., 2017) with a pre-trained Transformer encoder. In this approach, documents are segmented into passages, encoded using RoBERTa (Liu et al., 2019), and structured as fully connected subgraphs linked to a central node representing the document. A GAT captures multi-granularity document representations, while contrastive learning further enhances representation learning. While effective, this method does not learn the underlying graph topology. Rather, it relies on a fixed architecture and predefined connections.

Recent research explores integrating predefined static graph structures with language models to enhance document representation learning by combining local relational modeling with deep contextual encoding. One such study (Huang et al., 2022) proposes a unified model combining Graph Neural Network (GNN) models and BERT (Devlin et al., 2019) to mitigate the overemphasis on content-specific word usages. The method employs a sub-word graph to learn fine-grained syntactic relationships. Similarly, Onan (2023) introduce a hierarchical graph-based framework where BERT encodes contextual information at the node level, enhancing classification performance.

162 In multi-label classification, Liu et al. (2025) use XLNet (Yang et al., 2019) embeddings and generate a graph structure based on label co-occurrence, learning label correlations exclusively through graph attention. Moreover, class-specific and self-attention mechanisms enhance the model’s ability to capture contextual dependencies within the text.
 163
 164
 165

166 **Graph Structure Learning (GSL).** GSL (Franceschi et al., 2019; Chen et al., 2020) emerged as an alternative to heuristic-based graph constructions, whose manually specified rules often yield incomplete or task-misaligned topologies. GSL addresses these limitations by enabling parametric graph induction, wherein graph topology and node representations are jointly optimized.
 167
 168
 169
 170

171 Early approaches refine an initial graph using shallow feature embeddings and typically follow a metric-based method. Among them, IDGL (Chen et al., 2020) iteratively infers edges via node embedding similarity, while SE-GSL (Zou et al., 2023) applies an entropy-based abstraction to form hierarchical communities. More recent work leverages large language models (LLMs) to reduce reliance on explicit graph structural information as supervision signals. GraphEdit (Guo et al., 2024) uses instruction-tuning to fine-tune an LLM to predict edge relevance from node text, whereas LLaTA (Zhang et al., 2025) leverages tree-based in-context learning to integrate topology and text insights. While incorporating external knowledge improves robustness against noisy input graphs, such methods suffer from substantial computational inefficiencies, limiting their scalability to large graphs. Moreover, most GSL methods target non-textual domains such as citation and social networks (Franceschi et al., 2019; Chen et al., 2020; Zou et al., 2023). When applied to text, they generally operate on corpus-level graphs, treating each document as a node. This formulation neglects the semantic dependencies across text granularities, thereby restricting applicability to short or structurally simple documents. Moreover, graph structure learning in these cases is jointly optimized with the underlying graph encoder, thereby coupling the learned structure with model-specific inductive biases.
 172
 173
 174
 175
 176
 177
 178
 179
 180
 181
 182
 183
 184
 185

186 Despite the growing use of graph-based methods, the challenge of automatically learning graph topologies for document representation directly from raw text remains largely unexplored. Recent efforts underscore the effectiveness of integrating attention mechanisms and pre-trained language models for robust and adaptive graph-based document representations, while also highlighting the limitations of heuristic-based graph constructions—particularly in handling diverse domains and coping with modern document processing requirements such as large-scale data, long-range dependencies, and noisy and imbalanced data.
 187
 188
 189
 190
 191
 192
 193

194 3 LEARNING DATA-DRIVEN DOCUMENT GRAPHS

195
 196 We introduce a novel approach for learning data-driven graph structures, eliminating the reliance on manual graph design and minimizing domain dependency. Building upon insights from previous work (Xu et al., 2021; Liu et al., 2025) highlighting the capabilities of pre-trained language models and attention mechanisms for capturing contextual relationships (Voita et al., 2019; Clark et al., 2019), our methodology constructs homogeneous weighted graphs, where sentences serve as nodes and inter-sentence dependencies are learned via a self-attention mechanism.
 197
 198
 199
 200
 201
 202

203 **Motivation for Attention-Based Graphs.** Self-attention computes pairwise relevance scores between representational units conditioned on task supervision. Let D be a document with L sentences s_1, s_2, \dots, s_L , $X \in R^{L \times d}$ the sentence embedding matrix, and $\alpha = \text{Attn}(X) \in R^{L \times L}$ the resulting sentence-level attention matrix (aggregated across heads). Under mild assumptions, large entries α_{ij} indicate that s_j strongly influences s_i ’s contribution to the document-level prediction. Thus, thresholding α yields a data-adaptive sparsified graph $G = (V, E)$, where $V = \{s_1, s_2, \dots, s_L\}$ and $E = \{(s_i, s_j) \mid \alpha_{ij} \geq \tau_i\}$, with each edge weighted by its corresponding attention score α_{ij} and τ_i denoting a pre-calculated attention threshold for every sentence $s_i \in D$. This allows the graph to capture functional rather than purely surface interactions, resulting in a lightweight alternative to domain-engineered topologies. Notably, the resulting topology adapts to each document, enabling different sparsity patterns even among texts with similar surface characteristics.
 204
 205
 206
 207
 208
 209
 210
 211
 212
 213

214 Our use of sentences as nodes is motivated by their proven effectiveness in capturing document structure and their scalability for long texts (Song et al., 2020). Furthermore, we generate homogeneous rather than heterogeneous graphs to avoid the computational overhead and reliance on external
 215

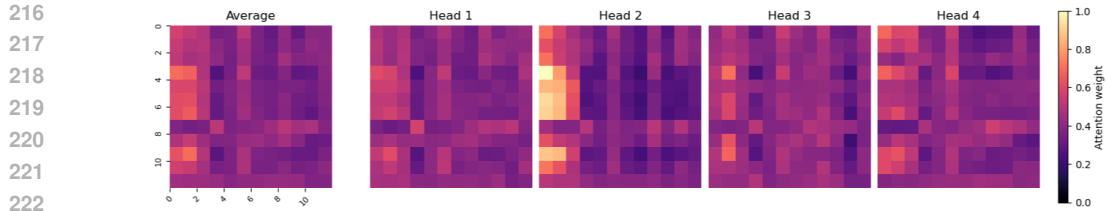


Figure 3: Learned attention weights averaged across heads for a randomly selected document from the BBC News dataset, consisting of 12 sentences.

tools (Sahu et al., 2019; Wang et al., 2023; Ai et al., 2025). Previous work also suggests that simpler graph constructions often perform better than more specialized ones (Bugueño & de Melo, 2023).

After learning the attention weights for all sentence pairs, a statistical filtering mechanism defines a minimum threshold for each row i (τ_i) in the attention matrix, ensuring that only strongly correlated sentence pairs (α_{ij}) are retained. This step also mitigates isolated nodes, enhancing the graph quality and reducing graph complexity. The overall framework is outlined in Figure 2, with a detailed description provided below.

3.1 DATA SEGMENTATION

To define the units that will serve as nodes within the learned graphs, namely, the sentences, our approach begins by segmenting the input document D into a sequence of its L preprocessed constituent sentences s_1, s_2, \dots, s_L . For this, we conduct a data-cleaning procedure followed by sentence tokenization.² Sentences containing fewer than five words are merged with the preceding one to prevent the graph size from growing excessively, ensure computational efficiency, and maintain meaningful sentence representations while reducing unnecessary complexity in graph construction. This segmentation allows the model to later capture sentence-level dependencies that are essential to accurately modeling the overall structure of the document graph.

3.2 LEARNING TASK-SPECIFIC DEPENDENCIES

Each sentence s_i is embedded into a fixed-dimensional vector $x_i \in \mathbb{R}^d$ using a pre-trained Sentence Transformer, with $d = 384$ in our experiments. The resulting set of embeddings x_1, x_2, \dots, x_L serves as the input representation of the document, effectively transforming the textual data into vector representations for further processing.

Building upon these representations, a multi-head self-attention model is trained to learn inter-sentence dependencies. The architecture comprises a multi-head attention mechanism, followed by a ReLU-activated non-linear layer, and concludes with a classification head designed to perform document classification across the available classes. Following recent findings (Wortsman et al., 2023), we substitute the conventional softmax activation function used during the scaled dot-product attention computation with a ReLU activation normalized by sequence length. This variant has been shown to yield a more efficient and effective attention mechanism (Bai et al., 2023; Zhao et al., 2024). The resulting learned attention matrix is given by α_{ij} for each sentence pair (s_i, s_j) . Motivated by prior work demonstrating that self-attention heads often correspond to interpretable linguistic patterns (Voita et al., 2019; Clark et al., 2019), we compute α_{ij} by averaging the attention matrices across all heads in the model (see Figure 3). Additional implementation details and visualizations of the resulting attention distributions are provided in Appendix B.

3.3 STATISTICAL FILTERING

To enhance the relevance of the attention weights produced by the multi-head self-attention model, we apply a statistical filtering step that selectively discards weak dependencies while retaining salient sentence pairs (α_{ij}) relevant to the classification task. This process effectively transforms attention weights into graph edges representing meaningful inter-sentence relationships. Filtering

²Implemented using the NLTK library in Python.

270 is conducted row-wise to prevent isolated nodes, establishing at least one edge per sentence, while
 271 self-loops are explicitly removed. Two alternative filtering strategies are introduced.
 272

273 **Mean-bound.** This approach computes the average attention score for each sentence s_i across
 274 all other sentences within the document and derives a minimum attention threshold incorporating a
 275 predefined tolerance degree δ . The threshold is given by:
 276

$$277 \quad \tau_i = \frac{1}{L} \sum_{j=1}^l \alpha_{ij} + \delta \cdot \text{std}(\alpha_i), \quad (1)$$

$$278$$

$$279$$

280 where $\text{std}(\alpha_i)$ is the standard deviation of the i -row of the learned attention matrix. This threshold
 281 is slightly greater than the mean, which reduces the tolerance level and decreases the number of
 282 retained entries in the attention matrix, thereby ensuring that only the most relevant dependencies
 283 are preserved.
 284

285 **Max-bound.** This strategy focuses on top-ranked dependencies, retaining attention scores proximate
 286 to the maximum observed value within each row, i.e., for each sentence s_i in the document.
 287 The threshold is calculated as:
 288

$$289 \quad \tau_i = \max_j(\alpha_{ij}) - \delta \cdot \text{std}(\alpha_i), \quad (2)$$

$$290$$

291 where $\text{std}(\alpha_i)$, as in Equation 1, is the standard deviation of the i -row of the learned attention matrix.
 292 Notably, we increase the tolerance for preserving entries around the peak attention score for each
 293 row, yielding a more aggressive pruning criterion.
 294

295 3.4 CONSOLIDATION

296 After statistical filtering, the resulting matrix is treated as the adjacency matrix of the learned graph.
 297 To ensure structural consistency, two operations account for special edge cases.
 298

299 **Sentence Merging.** When identical sentences occur at different positions in D , their corresponding
 300 edges are merged to maintain the integrity of the graph representation and better reflect the semantic
 301 structure of the document, while adjusting the set of effective sentence nodes in the final learned
 302 graph. For instance, in Figure 2, $s_3 = s_9$ in $D = \{s_1, s_2, \dots, s_{10}\}$. Therefore, their edges are
 303 unified, resulting in a reduced graph with nine unique sentence nodes.
 304

305 **Connectivity Preservation.** Isolated nodes need to be avoided. A typical scenario arises when
 306 there is no plausible edge for the row α_i (s_i) after statistical filtering, failing to establish meaningful
 307 connections. To address this, additional edges are introduced between s_i and its immediately pre-
 308 ceding and subsequent sentences. The attention weight associated with the self-loop α_{ii} is evenly
 309 distributed between these new edges, preserving the original attention-based weighting scheme.
 310

311 The final learned graph $G = (V, E)$ consists of unique sentence nodes $V \subseteq D$, encoded via Sentence
 312 Transformer embeddings, and undirected, attention-weighted edges E that effectively capture the
 313 document structure. More details about the graph induction from α are available in Appendix D.
 314

315 4 EXPERIMENTS

316 To study the merits of our learned graphs for document representation in various scenarios, we con-
 317 ducted experiments on three publicly available text classification datasets, comparing our approach
 318 against five heuristic-based construction schemes by training a GAT under consistent settings.
 319

320 4.1 DATASETS

321 We assess our model’s generalizability across balanced and unbalanced scenarios, covering topic
 322 classification and hyperpartisan news detection (see Table 1), using datasets of varying length: **BBC**
 323 **News**³ (Greene & Cunningham, 2006), a moderately imbalanced collection of English news articles
 324

³<http://derekgreene.com/bbc/>

324 Table 1: Statistics of datasets. Imbalance rate (IR) denotes the ratio of minority to majority classes.
325

Dataset	#Samples (train/val/test)	Avg. Length	#Classes	IR
BBC News	2,225 (1,547/177/443)	438 words (19 sent.)	5	4:5
HND	1,270 (516/129/625)	912 words (21 sent.)	2	1:2
arXiv	33,000 (28,000/2,500/2,500)	10,554 words (539 sent.)	11	1:2

330
331 in the areas of business, entertainment, politics, sport, and technology; **Hyperpartisan News Detec-**
332 **tion (HND)**⁴ (Kiesel et al., 2019) binary annotated for partisan bias; and **arXiv**⁵ (He et al., 2019), a
333 corpus of 33,000 scientific papers in physics, mathematics, computer science, and biology.

334 As BBC News lacks predefined data splits, we apply an 80/20 train–test partition, allocating 10% of
335 the training for validation. Duplicate entries are removed across all datasets. Further dataset details
336 are provided in Appendix A.
337

338 4.2 COMPARISON METHODS 339

340 **Heuristic-based Baselines.** We compare our learned graphs against five widely adopted heuristic-
341 based homogeneous graph constructions. While recent work also explores heterogeneous graphs
342 (Section 2.1), they differ fundamentally from our homogeneous setup and are not directly compara-
343 ble. In all baselines, graph nodes represent the unique sentences in a document D . We consider:

- 344 • **Complete Graph:** A fundamental baseline, where each sentence node is fully connected to all
345 others using unweighted edges, forming a complete graph.
- 346 • **Sentence Order:** Constructs undirected binary edges based on the natural order of sentence oc-
347 currence within the document. This approach solely captures the sequential structure of the text.
- 348 • **Window-based Co-Occurrence:** Undirected edges connect sentence nodes if they co-occur
349 within a fixed sliding window of size 3. Therefore, each sentence is connected to its two preced-
350 ing and two subsequent sentences. Notably, this construction can be considered a generalization
351 of the sentence order-based graph by capturing broader contextual dependencies.
- 352 • **Mean Semantic Similarity:** Defines weighted edges based on a cosine similarity threshold ap-
353 plied to the corresponding sentence embeddings. The threshold is computed as described in Equa-
354 tion 1, providing a fair comparison against our learned graphs.
- 355 • **Max Semantic Similarity:** Sets a higher cosine similarity threshold by following the procedure
356 outlined in Equation 2. It retains only the strongest connections, resulting in sparser graphs.
357

358 **Non-Graph Baselines.** We include strong non-graph baselines in Table 2 for com-
359 parative reference. We fine-tune **Longformer** (Beltagy et al., 2020) using the pre-
360 trained `longformer-base-4096`⁶ model with a sequence-classification head. **LongT5**
361 (Guo et al., 2022) is similarly fine-tuned using only the encoder of the pre-trained
362 `google/long-t5-tglobal-base`⁷ model, augmented with a linear classification head. We
363 additionally report previously published results for each dataset, including: fine-tuned **RoBERTa**
364 (Reusens et al., 2024; Liu et al., 2019) with Bayesian-optimized hyperparameters for BBC News;
365 **CogLTX** (Park et al., 2022; Ding et al., 2020), which selects informative sentences for document
366 classification, for HND; and **Llama3.2** (Li et al., 2025a; Touvron et al., 2023) for the arXiv dataset.
367 An extensive comparison including additional non-graph models is provided in Table 6. We further
368 implement a simple baseline that represents each document as the mean of its Sentence Transformer
369 embeddings, followed by a two-layer MLP (**SentenceEmb + MLP**). This model operates entirely
370 independently of graph structure and provides a controlled lower bound against which the gains
371 of our graph-based architectures can be assessed. We also report results from our sentence-level
372 self-attention models (**ReLUAttn-SentenceEmb + MLP**), which induce our learned graphs, as de-
373 scribed in Section 3.2.
374

⁴<https://zenodo.org/records/5776081>

⁵<https://huggingface.co/datasets/ccdv/arxiv-classification>

⁶<https://huggingface.co/allenai/longformer-base-4096>

⁷<https://huggingface.co/google/long-t5-tglobal-base>

378
379
380
381
382
383
384
385
386
387
388
389
390
391
392
393
394
395
396
397
398
399
400
401
402
403
404
405
406
407
408
409
410
411
412
413
414
415
416
417
418
419
420
421
422
423
424
425
426
427
428
429
430
431

Table 2: Classification performance of learned versus heuristic-based and non-graph models across datasets. Metrics include accuracy, macro-averaged F_1 score (mean \pm std. over 5 independent runs), graph statistics (average number of nodes, edges, and degree), and storage. Results for complete and mean semantic similarity baselines are excluded on arXiv due to excessive computational and runtime requirements. **Best**, second-best, and non-graph[†] results are highlighted as described. N/A entries indicate that the corresponding feature is not applicable (i.e., for non-graph models).

Scheme	Accuracy	F_1 -ma	$ V $	$ E $	Degree	Disk
<i>BBC News (2L-64U)</i>						
RoBERTa (Reusens et al., 2024) [†]	98.0	97.0	N/A	N/A	N/A	N/A
Longformer-base [†]	97.9 \pm 0.5	97.8 \pm 0.5	N/A	N/A	N/A	N/A
LongT5-tglobal-base [†]	96.3 \pm 0.5	96.3 \pm 0.5	N/A	N/A	N/A	N/A
SentenceEmb + MLP [†]	95.2 \pm 0.3	94.8 \pm 0.3	N/A	N/A	N/A	N/A
ReLUAttn-SentenceEmb + MLP [†]	95.9 \pm 0.4	95.7 \pm 0.4	N/A	N/A	N/A	N/A
Complete Graph	99.9 \pm 0.1	99.9 \pm 0.1	19.30	481.67	18.3	105MB
Sentence Order	99.7 \pm 0.3	99.7 \pm 0.4	19.30	36.61	1.87	74MB
Window Co-occurrence	99.8 \pm 0.3	99.8 \pm 0.4	19.30	71.21	3.62	76MB
Mean Semantic Similarity	99.4 \pm 0.5	99.3 \pm 0.6	19.30	159.68	5.40	84MB
Max Semantic Similarity	99.7 \pm 0.2	99.7 \pm 0.2	19.30	36.66	1.88	74MB
Learned Mean-Bound	99.9 \pm 0.1	99.9 \pm 0.1	19.30	213.80	8.26	90MB
Learned Max-Bound	99.6 \pm 0.5	99.6 \pm 0.5	19.30	60.27	3.04	77MB
<i>HND (3L-64U)</i>						
CogLTX (Park et al., 2022) [†]	94.8	Not Reported	N/A	N/A	N/A	N/A
Longformer-base [†]	85.4 \pm 1.0	85.3 \pm 1.0	N/A	N/A	N/A	N/A
LongT5-tglobal-base [†]	74.6 \pm 1.7	74.5 \pm 1.7	N/A	N/A	N/A	N/A
SentenceEmb + MLP [†]	74.8 \pm 1.0	74.7 \pm 1.0	N/A	N/A	N/A	N/A
ReLUAttn-SentenceEmb + MLP [†]	75.4 \pm 0.7	75.3 \pm 0.7	N/A	N/A	N/A	N/A
Complete Graph	94.6 \pm 1.2	94.5 \pm 1.2	19.48	710.55	18.48	70MB
Sentence Order	92.6 \pm 2.3	92.6 \pm 2.3	19.48	36.99	1.79	43MB
Window Co-occurrence	92.1 \pm 2.9	92.1 \pm 2.9	19.48	71.94	3.35	44MB
Mean Semantic Similarity	91.2 \pm 4.9	91.1 \pm 5.0	19.48	253.77	6.00	53MB
Max Semantic Similarity	92.8 \pm 5.5	92.8 \pm 5.6	19.48	36.93	1.78	43MB
Learned Mean-Bound	95.0 \pm 2.2	94.9 \pm 2.2	19.48	293.25	7.85	56MB
Learned Max-Bound	92.6 \pm 5.6	92.6 \pm 5.6	19.48	54.76	2.53	44MB
<i>arXiv (3L-64U)</i>						
Llama-3.2-1B-Instruct (Li et al., 2025a) [†]	89.2	89.0	N/A	N/A	N/A	N/A
Longformer-base [†]	86.9 \pm 0.8	86.7 \pm 0.7	N/A	N/A	N/A	N/A
LongT5-tglobal-base [†]	87.8 \pm 0.7	87.8 \pm 0.7	N/A	N/A	N/A	N/A
SentenceEmb + MLP [†]	79.9 \pm 0.3	79.1 \pm 0.3	N/A	N/A	N/A	N/A
ReLUAttn-SentenceEmb + MLP [†]	84.7 \pm 0.6	84.1 \pm 0.6	N/A	N/A	N/A	N/A
Sentence Order	87.8 \pm 0.5	87.3 \pm 0.5	510.33	1,034.28	2.02	25GB
Window Co-occurrence	87.9 \pm 1.9	87.4 \pm 2.0	510.33	2,064.93	4.03	26GB
Max Semantic Similarity	87.8 \pm 0.8	87.3 \pm 0.8	510.33	1,234.40	2.27	26GB
Learned Mean-Bound (10% train sample)	88.2 \pm 3.1	87.6 \pm 3.2	502.92	35,651.40	55.53	16GB
Learned Max-Bound (10% train sample)	91.7 \pm 1.9	91.3 \pm 2.1	502.92	1068.51	2.14	6GB
Learned Max-Bound (full data)	91.9 \pm 1.1	91.7 \pm 1.0	510.33	1082.22	2.14	25GB

4.3 EXPERIMENTAL SETUP

We established dataset-specific maximum sequence lengths to handle particularly long documents. While BBC News and HND retained full texts, a maximum of 1,800 sentences was set for arXiv, minimizing information loss and truncating less than 1.5% of document samples. To obtain sentence embeddings, we used the pre-trained Sentence Transformer `paraphrase-MiniLM-L6-v2`⁸. The tolerance degree δ is fixed at 0.5 throughout all experiments.

Self-Attention Model: We employed a single-layer four-head multi-head self-attention model, trained with a batch size of 32 for up to 20 epochs; however, additional experiments with a two-layer architecture are reported in Table 4, Appendix B. Optimization was performed using Adam (Kingma & Ba, 2014) with an initial learning rate of 0.001, employing early stopping if the validation macro-averaged F_1 score did not improve for five consecutive epochs.

Graph Attention Network (GAT): We assessed GAT architectures with 1 to 3 hidden layers and node embedding sizes in {64, 128, 256}. Dropout (rate=0.2) was applied after each convolutional

⁸<https://huggingface.co/sentence-transformers/paraphrase-MiniLM-L6-v2>

432 layer, edge weights were used as edge attributes, and average pooling aggregated node embeddings.
 433 Final document representations were classified through a softmax layer. Training was conducted for
 434 up to 50 epochs with a batch size of 64, utilizing the Adam optimizer (Kingma & Ba, 2014) and an
 435 initial learning rate of 0.001. Early stopping was applied as in self-attention models.

436 **Language Models:** Longformer and LongT5 are trained with a learning rate of 2×10^{-5} , a maxi-
 437 mum of 10 epochs, and patience of 3. Due to the model size (148M and 109M parameters, respec-
 438 tively) and computational constraints, we set the maximum sequence lengths to 1024, 2048, and
 439 4096 for each dataset, while LongT5 uses a maximum length of 5120 for arXiv. Batch size is fixed
 440 to 16.

441

442

443 5 RESULTS

444

445 Table 2 reports main results averaged over 5 runs, with accuracy and macro-averaged F_1 score
 446 accounting for class imbalance. Given the substantially longer documents in arXiv, GATs were
 447 first trained on 10% of the training samples for the learned graph variants (mean- and max-bound),
 448 and the best-performing model was subsequently scaled to the full dataset. GAT architectures were
 449 adapted to the dataset length: 2-layer GAT (64 units) for BBC News, and 3-layer GAT (64 units)
 450 for HND and arXiv, capturing the complex semantic relationships present in lengthy documents.
 451 Importantly, additional experiments using two alternative GNN backbones—Graph Convolutional
 452 Networks (GCN) (Kipf & Welling, 2017) and GraphSAGE (Hamilton et al., 2017)—are provided in
 453 Table 5; Appendix C.

454 All experiments were implemented in PyTorch Geometric on an NVIDIA GeForce RTX3050.

455

456 **Quality of the Results.** Learned graphs consistently outperform heuristic-based schemes across
 457 datasets, showing robust performance and proving competitive with non-graph methods, surpass-
 458 ing recent small language models. Gains over heuristic graphs are marginal on BBC News but
 459 become increasingly pronounced for longer documents. Notably, although the complete graph base-
 460 line matches the performance of our learned mean-bound graphs, it requires nearly twice the edges
 461 and 15 MB more storage. On HND, learned mean-bound graphs outperform the strongest heuristic
 462 baseline (max semantic similarity) by up to 2.1 F_1 points, with even larger improvements on arXiv
 463 (4.3 F_1 over window-based graphs, 2.7 F_1 over Llama-3.2). Remarkably, training on only 10% of
 464 the training data, our learned graphs outperform heuristic schemes and Longformer-base, with the
 465 max-bound variant surpassing Llama-3.2. These results emphasize the effectiveness of our method
 466 in capturing structural information in long texts.

467 Moreover, although ReLUAttn-SentenceEmb + MLP shows improvements over SentenceEmb +
 468 MLP, both methods perform well on mid-length documents but degrade substantially as length in-
 469 creases, highlighting the limitations of flat sentence pooling. In contrast, our learned graphs achieve
 470 consistent gains—reaching up to +20 F_1 on HND and +7 F_1 on arXiv. These findings indicate that
 471 modeling document structure, rather than relying solely on sentence-level content, is essential for
 472 long-text classification.

473

474 **Graph Structure Analysis.** A key advantage of our proposal is its ability to capture global con-
 475 textual dependencies within a document. Unlike heuristic graphs, which are limited to local context
 476 via fixed window sizes, our approach allows edges between distant but relevant sentences, consider-
 477 ing all sentences simultaneously and thereby enhancing the expressiveness of the learned structure.
 478 Despite comparable storage requirements and average degree, our learned mean-bound graphs sub-
 479 stantially outperform heuristic-based mean semantic similarity graphs. This indicates that the per-
 480 formance gains stem not from graph density but from the semantic relevance and structural alignment
 481 of the learned edges. On arXiv, even the strongest heuristic baselines (window co-occurrence and
 482 max semantic similarity graphs) exhibit higher average degrees than our learned max-bound graphs,
 483 yet achieve lower performance, underscoring the robustness and effectiveness of our approach.

484 Visualizations of adjacency matrices (Figure 4) underscore the importance of capturing comprehen-
 485 sive document structures, highlighting the significance of both initial and final sentences for accurate
 486 classification, particularly in long-form documents. For clarity, we include binarized versions of the
 487 learned adjacency matrices, as they typically exhibit lower edge weights than heuristic-based graphs.

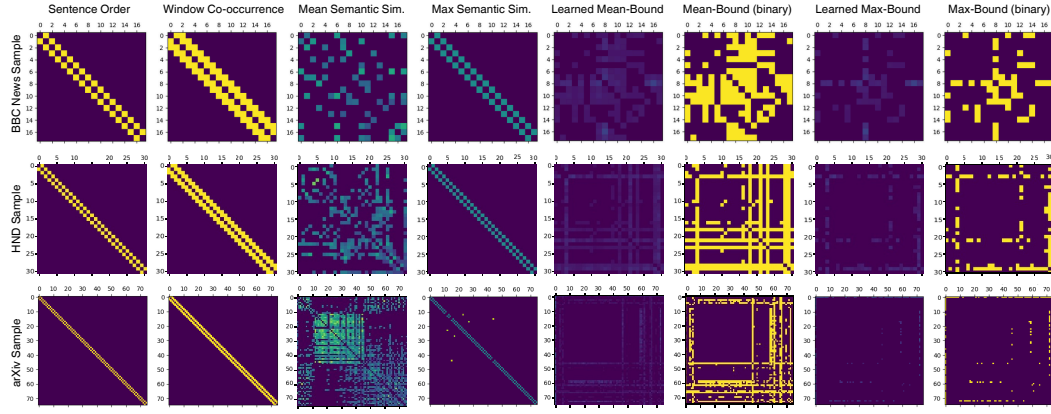


Figure 4: Adjacency matrix comparison across graph schemes on random dataset samples.

Table 3: Ablation results on the HND dataset.

δ	Mean-bound			Max-bound		
	F_1 -ma	Degree	Disk	F_1 -ma	Degree	Disk
0.25	93.4	11.47	61MB	94.0	2.40	44MB
0.50	94.9	8.86	57MB	92.6	2.79	45MB
0.75	94.8	6.78	53MB	91.6	3.29	45MB
1.00	90.7	5.20	50MB	94.2	3.90	46MB
—	No Filter: F_1 -ma: 89.6 / Degree: 39.96 / Disk: 104MB					

Ablation and Sensitivity Analysis. Table 3 reports the contribution of key design choices on the HND dataset: tolerance degree (δ), and filtering strategy. For mean-bound filtering, optimal performance is achieved with δ values between 0.5 and 0.75, with macro-averaged F_1 scores near 95%. In contrast, retaining all edges close to the row-wise mean attention score results in overly dense graphs (11.47 neighbors on average), leading to semantically noisy and undifferentiated message passing in the GAT, which degrades classification accuracy. This issue is more notorious when no filtering is applied and the full attention matrix is used as the adjacency matrix: The average node degree rises to nearly 40, and the F_1 score drops to 89.6%. Conversely, increasing the threshold to 1.0 substantially reduces the number of edges, proving insufficient for the task.

For the max-bound strategy, the GAT achieves competitive results by retaining only those edges close to the row-wise maximum attention value, with a considerable decay when increasing the tolerance degree. Notably, higher tolerance values in this setting retain more edges, in contrast to mean-bound, where higher thresholds produce sparser graphs. Interestingly, at $\delta = 1.0$, performance partially recovers, resembling the results obtained by mean-bound filtering with a higher average node degree.

These findings underscore the importance of statistical filtering to maintain a balance between graph sparsity and semantic relevance. They also suggest a need for further investigation into the interplay between edge semantics, node degree, and downstream task performance.

6 CONCLUSION

We introduced a data-driven framework that induces document graphs from supervised self-attention and prunes them via statistical filtering, eliminating reliance on domain-specific heuristics. Comprehensive experiments on three document classification datasets demonstrate that our learned graphs consistently outperform strong heuristic-based baselines, capturing the long-range and non-sequential dependencies that sentences may have among themselves. An ablation and sensitivity analysis confirms the importance of attention-guided sparsification and connectivity preservation. Future work includes adaptive threshold learning, additional tasks, and hierarchical extensions that incorporate multi-granular textual structure.

540 REFERENCES

542 Wei Ai, Ze Wang, Hongen Shao, Tao Meng, and Keqin Li. A multi-semantic passing framework for
 543 semi-supervised long text classification. *Applied Intelligence*, 53(17):20174–20190, 2023. doi:
 544 10.1007/s10489-023-04556-x.

545 Wei Ai, Jianbin Li, Ze Wang, Yingying Wei, Tao Meng, and Keqin Li. Contrastive multi-graph
 546 learning with neighbor hierarchical sifting for semi-supervised text classification. *Expert Systems
 547 with Applications*, 266, 2025. doi: 10.1016/j.eswa.2024.125952.

548 Yu Bai, Fan Chen, Huan Wang, Caiming Xiong, and Song Mei. Transformers as statisticians:
 549 Provable in-context learning with in-context algorithm selection. *Advances in Neural Information
 550 Processing Systems*, 36:57125–57211, 2023.

552 Iz Beltagy, Matthew E Peters, and Arman Cohan. Longformer: The long-document transformer.
 553 *arXiv preprint arXiv:2004.05150*, 2020.

554 Margarita Bugueño and Gerard de Melo. Connecting the dots: What graph-based text rep-
 555 resentations work best for text classification using graph neural networks? In *Findings of
 556 the Association for Computational Linguistics: EMNLP 2023*, pp. 8943–8960, 2023. doi:
 557 10.18653/v1/2023.findings-emnlp.600.

559 Margarita Bugueño, Hazem Abou Hamdan, and Gerard de Melo. Graphlss: Integrating lexical,
 560 structural, and semantic features for long document extractive summarization. *arXiv preprint
 561 arXiv:2410.21315*, 2024.

562 Esteban Castillo, Ofelia Cervantes, Darnes Vilarino, and D Báez-López. Author verification using a
 563 graph-based representation. *International Journal of Computer Applications*, 123(14):1–8, 2015.

565 Yu Chen, Lingfei Wu, and Mohammed Zaki. Iterative deep graph learning for graph neural net-
 566 works: Better and robust node embeddings. *Advances in neural information processing systems*,
 567 33:19314–19326, 2020.

568 Kevin Clark, Urvashi Khandelwal, Omer Levy, and Christopher D. Manning. What does BERT look
 569 at? an analysis of BERT’s attention. In Tal Linzen, Grzegorz Chrupała, Yonatan Belinkov, and
 570 Dieuwke Hupkes (eds.), *Proceedings of the 2019 ACL Workshop BlackboxNLP: Analyzing and
 571 Interpreting Neural Networks for NLP*, pp. 276–286, Florence, Italy, August 2019. Association for
 572 Computational Linguistics. doi: 10.18653/v1/W19-4828. URL <https://aclanthology.org/W19-4828/>.

574 Charles Condeau and Sébastien Harispe. Lsg attention: Extrapolation of pretrained transformers
 575 to long sequences. In Hisashi Kashima, Tsuyoshi Ide, and Wen-Chih Peng (eds.), *Advances in
 576 Knowledge Discovery and Data Mining*, pp. 443–454, Cham, 2023. Springer Nature Switzerland.
 577 ISBN 978-3-031-33374-3.

578 Peng Cui, Le Hu, and Yuanchao Liu. Enhancing extractive text summarization with topic-aware
 579 graph neural networks. In *Proceedings of the 28th International Conference on Computational
 580 Linguistics*, pp. 5360–5371, 2020. doi: 10.18653/v1/2020.coling-main.468.

582 Jacob Devlin, Ming-Wei Chang, Kenton Lee, and Kristina Toutanova. Bert: Bidirectional encoder
 583 representations from transformers. *arXiv preprint arXiv:1810.04805*, pp. 15, 2018.

584 Jacob Devlin, Ming-Wei Chang, Kenton Lee, and Kristina Toutanova. BERT: Pre-training of
 585 deep bidirectional transformers for language understanding. In *Proceedings of the 2019 Con-
 586 ference of the North American Chapter of the Association for Computational Linguistics: Hu-
 587 man Language Technologies, Volume 1 (Long and Short Papers)*, pp. 4171–4186, 2019. doi:
 588 10.18653/v1/N19-1423.

589 Ming Ding, Chang Zhou, Hongxia Yang, and Jie Tang. Cogltx: Applying bert to long texts. *Ad-
 590 vances in Neural Information Processing Systems*, 33:12792–12804, 2020.

591 Luca Franceschi, Mathias Niepert, Massimiliano Pontil, and Xiao He. Learning discrete structures
 592 for graph neural networks. In *International conference on machine learning*, pp. 1972–1982.
 593 PMLR, 2019.

594 Lukas Galke and Ansgar Scherp. Bag-of-Words vs. graph vs. sequence in text classification: Ques-
 595 tioning the necessity of text-graphs and the surprising strength of a wide MLP. In *Proceedings*
 596 *of the 60th Annual Meeting of the Association for Computational Linguistics (Volume 1: Long*
 597 *Papers)*, pp. 4038–4051, 2022. doi: 10.18653/v1/2022.acl-long.279.

598 Derek Greene and Pádraig Cunningham. Practical solutions to the problem of diagonal dominance
 599 in kernel document clustering. In *Proceedings of the 23rd international conference on Machine*
 600 *learning*, pp. 377–384, 2006.

602 Yongchun Gu, Yi Wang, Heng-Ru Zhang, Jiao Wu, and Xingquan Gu. Enhancing text classification
 603 by graph neural networks with multi-granular topic-aware graph. *IEEE Access*, 11:20169–20183,
 604 2023. doi: 10.1109/ACCESS.2023.3250109.

605 Mandy Guo, Joshua Ainslie, David C Uthus, Santiago Ontanon, Jianmo Ni, Yun-Hsuan Sung, and
 606 Yinfei Yang. Longt5: Efficient text-to-text transformer for long sequences. In *Findings of the*
 607 *Association for Computational Linguistics: NAACL 2022*, pp. 724–736, 2022.

609 Zirui Guo, Lianghao Xia, Yanhua Yu, Yuling Wang, Kangkang Lu, Zhiyong Huang, and Chao
 610 Huang. Graphedit: Large language models for graph structure learning. *arXiv preprint*
 611 *arXiv:2402.15183*, 2024.

613 Will Hamilton, Zhitao Ying, and Jure Leskovec. Inductive representation learning on large graphs.
 614 *Advances in neural information processing systems*, 30, 2017.

615 Samer Hassan and Carmen Banea. Random-walk term weighting for improved text classification. In
 616 *Proceedings of TextGraphs: the First Workshop on Graph Based Methods for Natural Language*
 617 *Processing*, pp. 53–60, 2006.

619 Jun He, Liqun Wang, Liu Liu, Jiao Feng, and Hao Wu. Long document classification from local
 620 word glimpses via recurrent attention learning. *IEEE Access*, 7:40707–40718, 2019. doi: 10.
 621 1109/ACCESS.2019.2907992.

623 Yibo Hu, MohammadSaleh Hosseini, Erick Skorupa Parolin, Javier Osorio, Latifur Khan, Patrick
 624 Brandt, and Vito D’Orazio. ConfliBERT: A pre-trained language model for political conflict
 625 and violence. In Marine Carpuat, Marie-Catherine de Marneffe, and Ivan Vladimir Meza Ruiz
 626 (eds.), *Proceedings of the 2022 Conference of the North American Chapter of the Association*
 627 *for Computational Linguistics: Human Language Technologies*, pp. 5469–5482, Seattle, United
 628 States, July 2022. Association for Computational Linguistics. doi: 10.18653/v1/2022.naacl-main.
 629 400. URL <https://aclanthology.org/2022.naacl-main.400/>.

630 Lianzhe Huang, Dehong Ma, Sujian Li, Xiaodong Zhang, and Houfeng Wang. Text level graph neu-
 631 ral network for text classification. In *Proceedings of the 2019 Conference on Empirical Methods*
 632 *in Natural Language Processing and the 9th International Joint Conference on Natural Language*
 633 *Processing*, pp. 3444–3450, 2019. doi: 10.18653/v1/D19-1345.

634 Yen-Hao Huang, Yi-Hsin Chen, and Yi-Shin Chen. ConTextING: Granting document-wise context-
 635 ual embeddings to graph neural networks for inductive text classification. In *Proceedings of the*
 636 *29th International Conference on Computational Linguistics*, pp. 1163–1168, 2022.

638 Johannes Kiesel, Maria Mestre, Rishabh Shukla, Emmanuel Vincent, Payam Adineh, David Cor-
 639 ney, Benno Stein, and Martin Potthast. SemEval-2019 task 4: Hyperpartisan news detection.
 640 In Jonathan May, Ekaterina Shutova, Aurelie Herbelot, Xiaodan Zhu, Marianna Apidianaki, and
 641 Saif M. Mohammad (eds.), *Proceedings of the 13th International Workshop on Semantic Evalua-
 642 tion*, pp. 829–839, Minneapolis, Minnesota, USA, June 2019. Association for Computational Lin-
 643 guistics. doi: 10.18653/v1/S19-2145. URL <https://aclanthology.org/S19-2145/>.

644 Diederik P Kingma and Jimmy Ba. Adam: A method for stochastic optimization. *arXiv preprint*
 645 *arXiv:1412.6980*, 2014.

646 Thomas N. Kipf and Max Welling. Semi-supervised classification with graph convolutional net-
 647 works, 2017. URL <https://arxiv.org/abs/1609.02907>.

648 Jonathan Li, Will Aitken, Rohan Bhambhoria, and Xiaodan Zhu. Prefix propagation: Parameter-
 649 efficient tuning for long sequences. In Anna Rogers, Jordan Boyd-Graber, and Naoaki Okazaki
 650 (eds.), *Proceedings of the 61st Annual Meeting of the Association for Computational Linguistics*
 651 (*Volume 2: Short Papers*), pp. 1408–1419, Toronto, Canada, July 2023a. Association for Compu-
 652 tational Linguistics. doi: 10.18653/v1/2023.acl-short.120. URL <https://aclanthology.org/2023.acl-short.120/>.

653

654 Lujun Li, Lama Sleem, Niccolò Gentile, Geoffrey Nichil, and Radu State. Small language models
 655 in the real world: Insights from industrial text classification, 2025a. URL <https://arxiv.org/abs/2505.16078>.

656

657 Pengyi Li, Xueying Fu, Juntao Chen, and Junyi Hu. CoGraphNet for enhanced text classification
 658 using word-sentence heterogeneous graph representations and improved interpretability. *Scientific*
 659 *Reports*, 15(1):356, 2025b. doi: 10.1038/s41598-024-83535-9.

660

661 Wenzhe Li and Nikolaos Aletras. Improving graph-based text representations with character and
 662 word level n-grams. In *Proceedings of the 2nd Conference of the Asia-Pacific Chapter of the*
 663 *Association for Computational Linguistics and the 12th International Joint Conference on Natural*
 664 *Language Processing (Volume 2: Short Papers)*, pp. 228–233, 2022. doi: 10.18653/v1/2022.
 665 *aacl-short.29*.

666

667 Xianming Li, Zongxi Li, Xiaotian Luo, Haoran Xie, Xing Lee, Yingbin Zhao, Fu Lee Wang, and
 668 Qing Li. Recurrent attention networks for long-text modeling. In Anna Rogers, Jordan Boyd-
 669 Gruber, and Naoaki Okazaki (eds.), *Findings of the Association for Computational Linguistics:*
 670 *ACL 2023*, pp. 3006–3019, Toronto, Canada, July 2023b. Association for Computational Linguistics.
 671 doi: 10.18653/v1/2023.findings-acl.188. URL <https://aclanthology.org/2023.findings-acl.188/>.

672

673 Ximing Li, Bing Wang, Yang Wang, and Meng Wang. Graph-based text classification by contrastive
 674 learning with text-level graph augmentation. *ACM Transactions on Knowledge Discovery from*
 675 *Data*, 18(4):1–21, 2024. doi: 10.1145/3638353.

676

677 Yinhan Liu, Myle Ott, Naman Goyal, Jingfei Du, Mandar Joshi, Danqi Chen, Omer Levy, Mike
 678 Lewis, Luke Zettlemoyer, and Veselin Stoyanov. Roberta: A robustly optimized bert pretraining
 679 approach. *arXiv preprint arXiv:1907.11692*, 2019.

680

681 Zhi Liu, Yunjie Huang, Xincheng Xia, and Yihao Zhang. All is attention for multi-label text
 682 classification. *Knowledge and Information Systems*, 67(2):1249–1270, 2025. doi: 10.1007/s10115-024-02253-w.

683

684 Rada Mihalcea and Paul Tarau. TextRank: Bringing order into text. In *Proceedings of the 2004*
 685 *Conference on Empirical Methods in Natural Language Processing*, pp. 404–411, 2004.

686

687 Mohammad Mohammadi and Sreejita Ghosh. A prototype-based model for set classification, 2025.
 688 URL <https://arxiv.org/abs/2408.13720>.

689

690 Aytuğ Onan. Hierarchical graph-based text classification framework with contextual node embed-
 691 ding and bert-based dynamic fusion. *Journal of King Saud University-Computer and Information*
 692 *Sciences*, 35(7), 2023. doi: 10.1016/j.jksuci.2023.101610.

693

694 Hyunji Park, Yogarshi Vyas, and Kashif Shah. Efficient classification of long documents using
 695 transformers. In Smaranda Muresan, Preslav Nakov, and Aline Villavicencio (eds.), *Proceed-
 696 ings of the 60th Annual Meeting of the Association for Computational Linguistics (Volume 2:*
 697 *Short Papers*), pp. 702–709, Dublin, Ireland, May 2022. Association for Computational Lin-
 698 *guistics*. doi: 10.18653/v1/2022.acl-short.79. URL <https://aclanthology.org/2022.acl-short.79/>.

699

700 Jeffrey Pennington, Richard Socher, and Christopher D Manning. Glove: Global vectors for word
 701 representation. In *Proceedings of the 2014 conference on empirical methods in natural language*
 702 *processing (EMNLP)*, pp. 1532–1543, 2014.

703

704 Colin Raffel, Noam Shazeer, Adam Roberts, Katherine Lee, Sharan Narang, Michael Matena, Yanqi
 705 Zhou, Wei Li, and Peter J Liu. Exploring the limits of transfer learning with a unified text-to-text
 706 transformer. *Journal of machine learning research*, 21(140):1–67, 2020.

702 Manon Reusens, Alexander Stevens, Jonathan Tonglet, Johannes De Smedt, Wouter Verbeke, Seppe
 703 vanden Broucke, and Bart Baesens. Evaluating text classification: A benchmark study. *Expert
 704 Systems with Applications*, 254:124302, 2024. ISSN 0957-4174. doi: <https://doi.org/10.1016/j.eswa.2024.124302>. URL <https://www.sciencedirect.com/science/article/pii/S0957417424011680>.

707 François Rousseau, Emmanouil Kiagias, and Michalis Vazirgiannis. Text categorization as a graph
 708 classification problem. In *Proceedings of the 53rd Annual Meeting of the Association for Compu-
 709 tational Linguistics and the 7th International Joint Conference on Natural Language Processing
 710 (Volume 1: Long Papers)*, pp. 1702–1712, 2015. doi: 10.3115/v1/P15-1164.

711 Sunil Kumar Sahu, Fenia Christopoulou, Makoto Miwa, and Sophia Ananiadou. Inter-sentence re-
 712 lation extraction with document-level graph convolutional neural network. In Anna Korhonen,
 713 David Traum, and Lluís Màrquez (eds.), *Proceedings of the 57th Annual Meeting of the Associa-
 714 tion for Computational Linguistics*, pp. 4309–4316, Florence, Italy, July 2019. Association for
 715 Computational Linguistics. doi: 10.18653/v1/P19-1423. URL <https://aclanthology.org/P19-1423/>.

716 Ksh. Nareshkumar Singh, S. Dickeeta Devi, H. Mamata Devi, and Anjana Kakoti Mahanta. A
 717 novel approach for dimension reduction using word embedding: An enhanced text classifica-
 718 tion approach. *International Journal of Information Management Data Insights*, 2(1):100061,
 719 2022. ISSN 2667-0968. doi: <https://doi.org/10.1016/j.jjimei.2022.100061>. URL <https://www.sciencedirect.com/science/article/pii/S2667096822000052>.

720 Wei Song, Ziyao Song, Ruiji Fu, Lizhen Liu, Miaomiao Cheng, and Ting Liu. Discourse self-
 721 attention for discourse element identification in argumentative student essays. In Bonnie Web-
 722 ber, Trevor Cohn, Yulan He, and Yang Liu (eds.), *Proceedings of the 2020 Conference on Em-
 723 pirical Methods in Natural Language Processing (EMNLP)*, pp. 2820–2830, Online, November
 724 2020. Association for Computational Linguistics. doi: 10.18653/v1/2020.emnlp-main.225. URL
 725 <https://aclanthology.org/2020.emnlp-main.225/>.

726 Hugo Touvron, Thibaut Lavril, Gautier Izacard, Xavier Martinet, Marie-Anne Lachaux, Timothée
 727 Lacroix, Baptiste Rozière, Naman Goyal, Eric Hambro, Faisal Azhar, et al. Llama: Open and
 728 efficient foundation language models. *arXiv preprint arXiv:2302.13971*, 2023.

729 Petar Veličković, Guillem Cucurull, Arantxa Casanova, Adriana Romero, Pietro Lio, and Yoshua
 730 Bengio. Graph attention networks. *arXiv preprint arXiv:1710.10903*, 2017.

731 Elena Voita, David Talbot, Fedor Moiseev, Rico Sennrich, and Ivan Titov. Analyzing multi-head
 732 self-attention: Specialized heads do the heavy lifting, the rest can be pruned. In Anna Korhonen,
 733 David Traum, and Lluís Màrquez (eds.), *Proceedings of the 57th Annual Meeting of the Associa-
 734 tion for Computational Linguistics*, pp. 5797–5808, Florence, Italy, July 2019. Association for
 735 Computational Linguistics. doi: 10.18653/v1/P19-1580. URL <https://aclanthology.org/P19-1580/>.

736 Kunze Wang, Yihao Ding, and Soyeon Caren Han. Graph neural networks for text classification: A
 737 survey. *Artificial Intelligence Review*, 57(8):190, 2024.

738 Yizhao Wang, Chenxi Wang, Jieyu Zhan, Wenjun Ma, and Yuncheng Jiang. Text fcg: Fusing con-
 739 textual information via graph learning for text classification. *Expert Systems with Applications*,
 740 219:119658, 2023. doi: 10.1016/j.eswa.2024.125952.

741 Benjamin Warner, Antoine Chaffin, Benjamin Clavié, Orion Weller, Oskar Hallström, Said
 742 Taghadouini, Alexis Gallagher, Raja Biswas, Faisal Ladhak, Tom Aarsen, et al. Smarter, bet-
 743 ter, faster, longer: A modern bidirectional encoder for fast, memory efficient, and long context
 744 finetuning and inference. *arXiv preprint arXiv:2412.13663*, 2024.

745 Mitchell Wortsman, Jaehoon Lee, Justin Gilmer, and Simon Kornblith. Replacing softmax with relu
 746 in vision transformers. *arXiv preprint arXiv:2309.08586*, 2023.

747 Peng Xu, Xinchi Chen, Xiaofei Ma, Zhiheng Huang, and Bing Xiang. Contrastive document rep-
 748 resentation learning with graph attention networks. In *Findings of the Association for Compu-
 749 tational Linguistics: EMNLP 2021*, pp. 3874–3884, 2021. doi: 10.18653/v1/2021.findings-emnlp.
 750 327.

756 Zhilin Yang, Zihang Dai, Yiming Yang, Jaime Carbonell, Russ R Salakhutdinov, and Quoc V Le.
 757 Xlnet: Generalized autoregressive pretraining for language understanding. *Advances in Neural*
 758 *Information Processing Systems*, 32, 2019.

759

760 Liang Yao, Chengsheng Mao, and Yuan Luo. Graph convolutional networks for text classification.
 761 *Proceedings of the AAAI Conference on Artificial Intelligence*, 33:7370–7377, 2019. doi: 10.
 762 1609/aaai.v33i01.33017370.

763 Jungmin Yun, Miheon Kim, and Youngbin Kim. Focus on the core: Efficient attention via
 764 pruned token compression for document classification. In Houda Bouamor, Juan Pino, and
 765 Kalika Bali (eds.), *Findings of the Association for Computational Linguistics: EMNLP 2023*,
 766 pp. 13617–13628, Singapore, December 2023. Association for Computational Linguistics.
 767 doi: 10.18653/v1/2023.findings-emnlp.909. URL <https://aclanthology.org/2023.findings-emnlp.909/>.

768

769 Yufeng Zhang, Xueli Yu, Zeyu Cui, Shu Wu, Zhongzhen Wen, and Liang Wang. Every docu-
 770 ment owns its structure: Inductive text classification via graph neural networks. In Dan Ju-
 771 rafsky, Joyce Chai, Natalie Schluter, and Joel Tetreault (eds.), *Proceedings of the 58th An-
 772 nual Meeting of the Association for Computational Linguistics*, pp. 334–339, Online, July
 773 2020. Association for Computational Linguistics. doi: 10.18653/v1/2020.acl-main.31. URL
 774 <https://aclanthology.org/2020.acl-main.31/>.

775

776 Zhihan Zhang, Xunkai Li, Zhu Lei, Guang Zeng, Ronghua Li, and Guoren Wang. Rethinking graph
 777 structure learning in the era of llms, 2025. URL <https://arxiv.org/abs/2503.21223>.

778

779 Yang Zhao, Yanwu Xu, Zhisheng Xiao, Haolin Jia, and Tingbo Hou. MobileDiffusion: Instant
 780 text-to-image generation on mobile devices. In *European Conference on Computer Vision*, pp.
 225–242. Springer, 2024.

781

782 Yukun Zhu, Ryan Kiros, Rich Zemel, Ruslan Salakhutdinov, Raquel Urtasun, Antonio Torralba, and
 783 Sanja Fidler. Aligning books and movies: Towards story-like visual explanations by watching
 784 movies and reading books. In *Proceedings of the IEEE international conference on computer
 vision*, pp. 19–27, 2015.

785

786 Dongcheng Zou, Hao Peng, Xiang Huang, Renyu Yang, Jianxin Li, Jia Wu, Chunyang Liu, and
 787 Philip S Yu. Se-gsl: A general and effective graph structure learning framework through structural
 788 entropy optimization. In *Proceedings of the ACM Web Conference 2023*, pp. 499–510, 2023.

789

790 A DATASETS 791

792 **BBC News**⁹ (Greene & Cunningham, 2006): A moderately imbalanced collection of 2,225 English
 793 documents from the BBC News website (2004–2005) in the areas of business, entertainment, poli-
 794 tics, sport, and technology. As BBC News lacks predefined data splits, after duplicate removal, we
 795 partition the data into training (1,547), validation (177), and test (443) sets. Notably, the dataset is
 796 available for non-commercial and research purposes only.

797 **Hyperpartisan News Detection (HND)**¹⁰ (Kiesel et al., 2019): English news articles labeled ac-
 798 cording to whether they show blind or unreasoned allegiance to a single political party or entity, or
 799 not. Although it comprises two parts, `byarticle` and `bypublisher`, we use the first one with
 800 645 training and 625 test samples labeled through crowdsourcing. As HND does not have a prede-
 801 fined validation split, we reserve 10% of the training samples for such a purpose. The collection is
 802 licensed under a Creative Commons Attribution 4.0 International License.

803 **arXiv**¹¹ (He et al., 2019): A collection of 33,000 very long scientific papers in physics, mathematics,
 804 computer science, and biology sourced from arXiv. The documents were originally obtained in PDF
 805 format and subsequently converted into plain text using the arXiv sanity preserver tool¹². The corpus

806 ⁹<http://derekgreen.com/bbc/>

807 ¹⁰<https://zenodo.org/records/5776081>

808 ¹¹<https://huggingface.co/datasets/ccdv/arxiv-classification>

809 ¹²<https://github.com/karpathy/arxiv-sanity-preserver/>

810 is organized into 11 classes with a slight class imbalance, and partitioned into three splits: train
 811 (28,000), validation (2,500), and test (2,500).
 812

813 B SELF-ATTENTION FORMULATION

814 B.1 RELU-BASED ATTENTION

817 Self-attention provides a mechanism for modeling long-range dependencies by enabling each token
 818 in a sequence to attend to all others, thus producing non-local contextualized representations. This is
 819 achieved by projecting the input into three parameterized spaces (queries (Q), keys (K), and values
 820 (V)) which define pairwise interactions across tokens. Classical self-attention computes token-level
 821 similarity scores via scaled dot-products between queries and keys, followed by a nonlinear trans-
 822 formation (typically softmax) that yields normalized attention weights. These weights are then used
 823 to aggregate information from the values, producing context-aware token embeddings. Formally, a
 824 single-head self-attention mechanism is often written as:

$$825 \quad \alpha = \text{Attn} = \phi \left(\frac{QK^T}{\sqrt{d_k}} \right) V, \quad (3)$$

826 where $\phi(\cdot)$ denotes the nonlinear activation (softmax in the standard formulation), $d_k = \frac{d}{H}$ is the
 827 head dimension, and H heads are used in parallel to form multi-head self-attention.
 828

829 In our setting, let be $X \in \mathbb{R}^{L \times d}$ denote the input representation of a document with at most L
 830 sentence-tokens, each embedded into a d -dimensional space (e.g., $d = 384$ using the Sentence
 831 Transformer).

832 We obtain queries, keys, and values via linear projections of X :

$$833 \quad q, k, v = XW_{q,k,v} + b_{q,k,v} \in \mathbb{R}^{L \times d}, \quad (4)$$

834 where $W_{q,k,v} \in \mathbb{R}^{d \times d}$ and $b_{q,k,v} \in \mathbb{R}^d$.

835 These are then reshaped and partitioned into per-head matrices $Q, K, V \in \mathbb{R}^{H \times L \times d_k}$, so that for
 836 each head $h \in \{1, \dots, H\}$ we have:

$$837 \quad Q^h, K^h, V^h \in \mathbb{R}^{L \times d_k}. \quad (5)$$

838 Afterwards, we compute the scaled-dot product attention logits for each head:

$$839 \quad S^h = \frac{1}{\sqrt{d_k}} Q^h (K^h)^T \in \mathbb{R}^{L \times L}. \quad (6)$$

840 Unlike the softmax formulation, we employ the element-wise ReLU activation as the non-linearity,
 841 which is normalized by sequence length L :

$$842 \quad \alpha_{ij}^h = \frac{\text{ReLU}(S_{ij}^h)}{L}, \quad i, j \in \{1, \dots, L\}, \quad (7)$$

843 yielding a non-negative but not necessarily stochastic attention distribution.

844 Once the attention logits are obtained, the final head-averaged attention map is given by:

$$845 \quad \alpha = \frac{1}{H} \sum_{h=1}^H \alpha^h \in \mathbb{R}^{L \times L}. \quad (8)$$

846 Head-specific outputs are computed as weighted value combinations, which are then concatenated
 847 to obtain the final output projection:

$$848 \quad \begin{aligned} O^h &= \alpha^h V^h & \in \mathbb{R}^{L \times d_k}, \\ 849 O &= \text{Concat}(O^1, \dots, O^H) & \in \mathbb{R}^{L \times d}, \\ 850 Y &= OW_o + b_o & \in \mathbb{R}^{L \times d}, \end{aligned} \quad (9)$$

Table 4: Results of a 1- and a 2-layer four-head multi-head self-attention model.

		1-layer		2-layer	
		Acc	F ₁ -ma	Acc	F ₁ -ma
BBC News	sport	-	98.7	-	99.1
	entertainment	-	95.2	-	92.9
	business	-	94.1	-	93.5
	tech	-	96.8	-	97.4
	politics	-	91.4	-	93.2
HND	macro-avg.	95.5	95.3	95.5	95.2
	non-hyperpartisan	-	75.5	-	76.4
	hyperpartisan	-	77.3	-	76.2
	macro-avg.	76.4	76.4	76.4	76.3

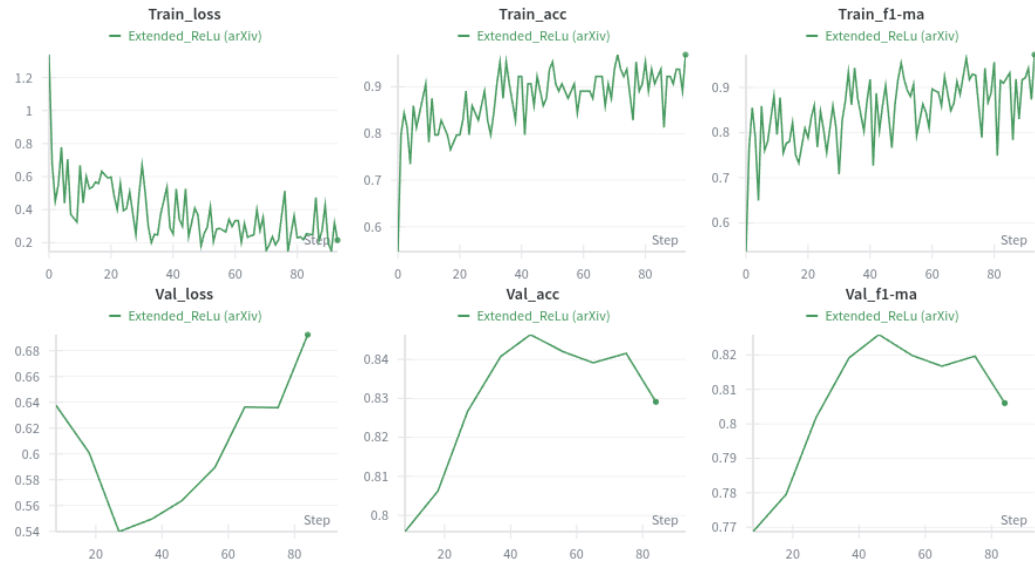


Figure 5: Learning curves of the 1-layer MHA model used for graph induction in the arXiv dataset.

where $W_o \in \mathbb{R}^{d \times d}$ and $b_o \in \mathbb{R}^d$ are learnable output projection parameters. The final document representation Y thus encodes each token with information aggregated from all others through ReLU-based multi-head self-attention.

For implementation details, please refer to our public repository: <https://github.com/available/upon/publication>.

B.2 ROBUSTNESS OF MULTI-HEAD SELF-ATTENTION MODEL

As Table 4 shows, our method demonstrates strong robustness across model architectures. Even shallow self-attention models induce strong document representations. Notably, it is essential for the learned attention weights to exhibit sparsity, which is critical for effectively identifying potential edges throughout the document. This sparsity facilitates the subsequent training of GAT models by efficiently exploring and leveraging the local neighborhood structure within the learned graph, enhancing its capacity to capture meaningful relationships within the document.

Model Convergence Figure 5 presents the learning curves of the multi-head attention model used to induce graphs for the arXiv dataset. While the training loss decreases steadily throughout the optimization process, the validation loss begins to rise after the initial training steps. Early stopping is therefore applied to preserve the model checkpoint that achieves the best validation performance, as described in Section 4.3.

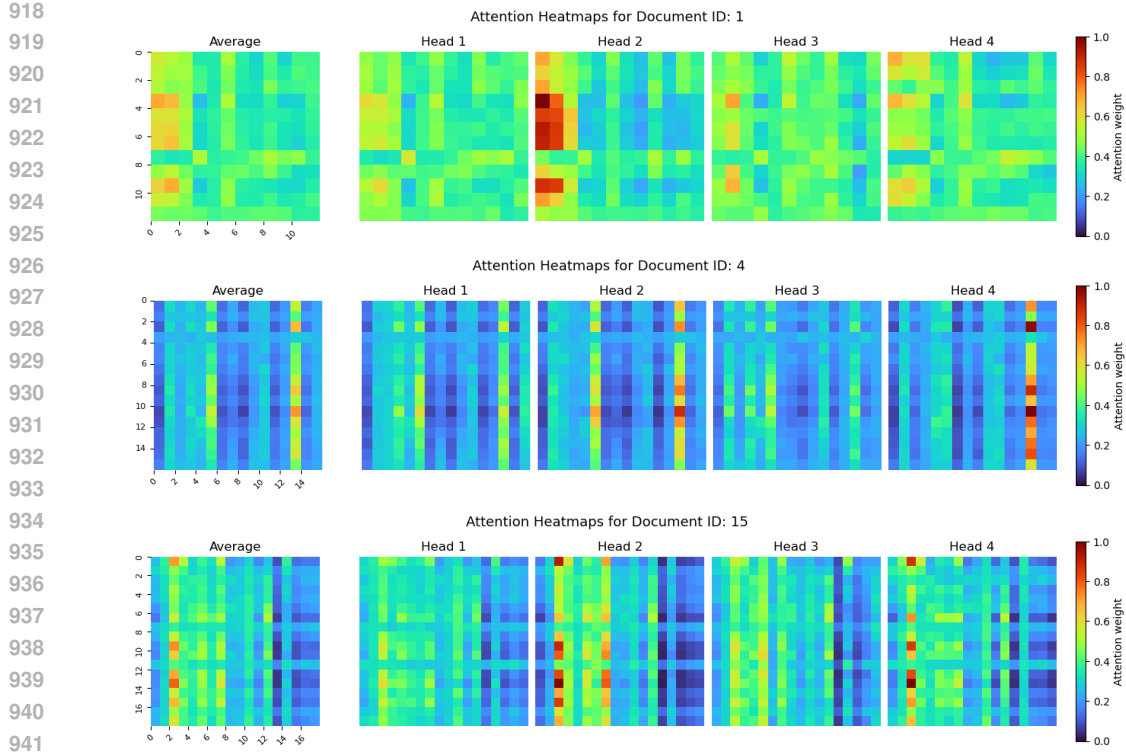


Figure 6: Learned attention weights for randomly selected samples from the BBC News dataset.

B.3 LEARNED ATTENTION DISTRIBUTIONS

Figure 6, Figure 7, and Figure 8 visualize, as heat maps, the attention-weight distributions learned by the self-attention models used for our graph induction process across the three datasets. A different colormap is employed than in Figure 2 and Figure 3 to enhance perceptual contrast, particularly for longer documents such as those in the arXiv corpus.

As described in Section 3.2, we average the attention matrices across heads to obtain a unified representation of the model’s learned dependencies. This averaging preserves patterns consistently identified as important across heads: when a head assigns a high weight to a sentence pair (s_i, s_j) , its contribution remains evident—albeit attenuated—in the aggregated matrix. In contrast, dependencies that are weak and detected by only a small subset of heads are further diminished through averaging, yielding values that approach zero.

C PERFORMANCE VARIABILITY ACROSS GNN BACKBONES

We conducted additional experiments varying the type of convolutional layer used in our graph encoder models, including Graph Attention Networks (**GAT**) (Veličković et al., 2017), Graph Convolutional Networks (**GCN**) (Kipf & Welling, 2017), and **GraphSAGE** (Hamilton et al., 2017). The results are reported in Table 5. The table shows that changing the underlying graph neural network architecture yields variable performance. However, GAT consistently outperforms both GCN and GraphSAGE across the three datasets examined in this work. Furthermore, we observe that our learned graphs consistently achieve higher performance than those constructed using heuristic methods, which emphasizes that the improvements stem from the graph-construction module rather than from the choice of GNN.

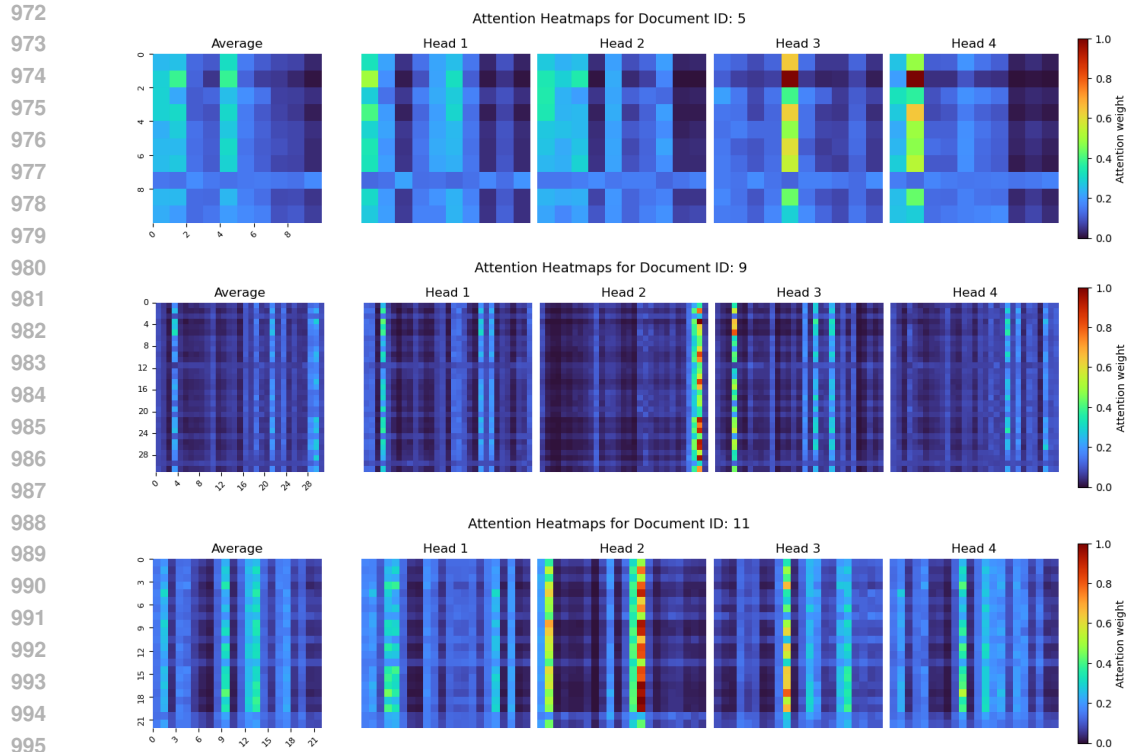


Figure 7: Learned attention weights for randomly selected samples from the HND dataset.

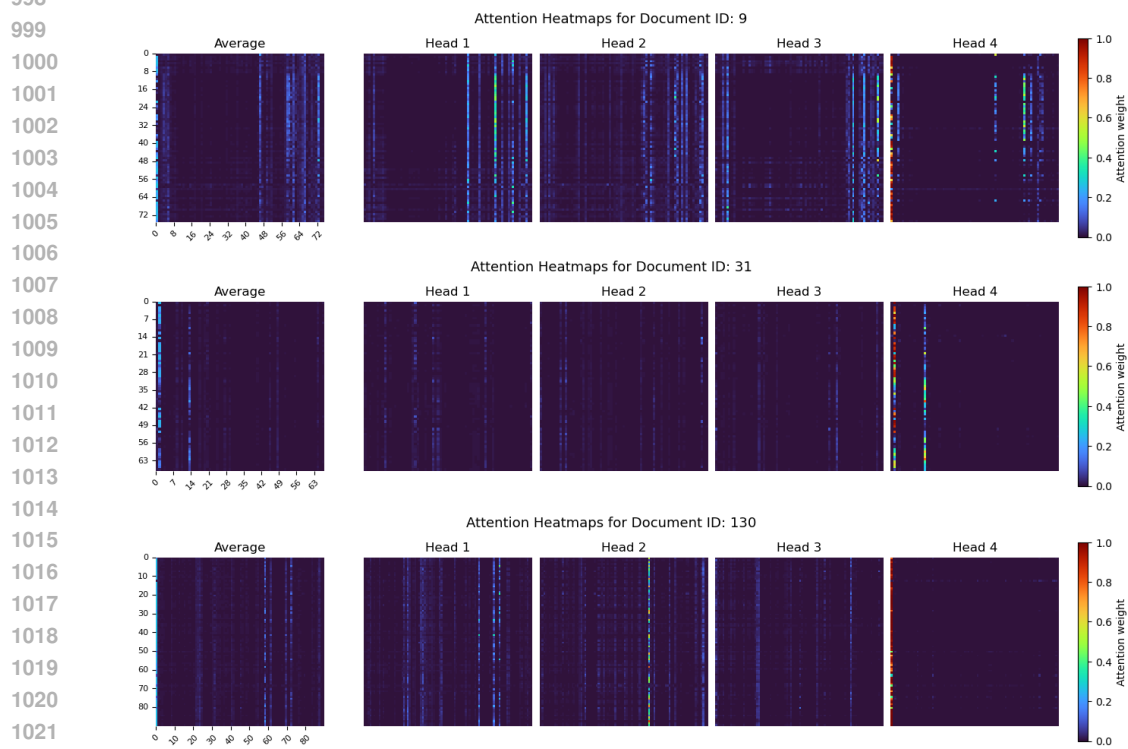


Figure 8: Learned attention weights for randomly selected samples from the arXiv dataset.

1026 Table 5: Classification performance of learned versus heuristic-based graphs across datasets. Re-
 1027 sults encompass three different encoder models, including Graph Attention Network (GAT), Graph
 1028 Convolutional Network (GCN), and GraphSAGE. Metrics include accuracy and macro-averaged F_1
 1029 score (mean \pm std. over 5 independent runs). Results for complete and mean semantic similarity
 1030 baselines are excluded on arXiv due to excessive computational and runtime requirements. **Best** and
 1031 second-best results for each GNN backbone, as well as the overall ***best** result at the dataset level,
 1032 are highlighted as described.

Scheme	GAT		GCN		GraphSAGE	
	Accuracy	$F_1\text{-ma}$	Accuracy	$F_1\text{-ma}$	Accuracy	$F_1\text{-ma}$
<i>BBC News (2L-64U)</i>						
Complete Graph	*99.9 \pm 0.1	*99.9 \pm 0.1	99.8 \pm 0.1	99.8 \pm 0.1	99.5 \pm 0.3	99.4 \pm 0.3
Sentence Order	99.7 \pm 0.3	99.7 \pm 0.4	99.1 \pm 0.4	99.1 \pm 0.4	99.6 \pm 0.2	99.6 \pm 0.2
Window Co-occurrence	99.8 \pm 0.3	99.8 \pm 0.4	98.4 \pm 1.1	98.3 \pm 1.2	99.0 \pm 0.5	98.9 \pm 0.6
Mean Semantic Similarity	99.4 \pm 0.5	99.3 \pm 0.6	99.4 \pm 0.5	99.4 \pm 0.5	98.8 \pm 0.6	98.8 \pm 0.7
Max Semantic Similarity	99.7 \pm 0.2	99.7 \pm 0.2	99.1 \pm 0.8	99.1 \pm 0.9	99.4 \pm 0.2	99.4 \pm 0.2
Learned Mean-Bound	*99.9 \pm 0.1	*99.9 \pm 0.1	99.5 \pm 0.2	99.4 \pm 0.2	98.5 \pm 0.7	98.4 \pm 0.7
Learned Max-Bound	99.6 \pm 0.5	99.6 \pm 0.5	99.1 \pm 0.3	99.1 \pm 0.3	98.8 \pm 0.7	98.8 \pm 0.7
<i>HND (3L-64U)</i>						
Complete Graph	94.6 \pm 1.2	94.5 \pm 1.2	92.3 \pm 3.5	92.3 \pm 3.5	91.0 \pm 4.0	91.0 \pm 4.0
Sentence Order	92.6 \pm 2.3	92.6 \pm 2.3	88.7 \pm 3.5	88.7 \pm 3.5	91.1 \pm 4.0	91.1 \pm 4.0
Window Co-occurrence	92.1 \pm 2.9	92.1 \pm 2.9	88.3 \pm 2.4	88.2 \pm 2.4	93.5 \pm 0.5	93.5 \pm 0.5
Mean Semantic Similarity	91.2 \pm 4.9	91.1 \pm 5.0	90.8 \pm 3.8	90.8 \pm 3.8	93.6 \pm 1.9	93.6 \pm 1.9
Max Semantic Similarity	92.8 \pm 5.5	92.8 \pm 5.6	91.8 \pm 3.5	91.8 \pm 3.5	92.4 \pm 3.9	92.4 \pm 4.0
Learned Mean-Bound	*95.0 \pm 2.2	*94.9 \pm 2.2	86.0 \pm 3.4	85.9 \pm 3.4	93.1 \pm 3.4	93.1 \pm 3.4
Learned Max-Bound	92.6 \pm 5.6	92.6 \pm 5.6	92.5 \pm 1.7	92.5 \pm 1.7	94.9 \pm 1.1	94.8 \pm 1.1
<i>arXiv (3L-64U)</i>						
Sentence Order	87.8 \pm 0.5	87.3 \pm 0.5	85.5 \pm 0.8	84.9 \pm 0.9	85.9 \pm 0.7	85.3 \pm 0.7
Window Co-occurrence	87.9 \pm 1.9	87.4 \pm 2.0	85.8 \pm 0.8	85.1 \pm 0.9	87.0 \pm 1.0	86.4 \pm 1.1
Max Semantic Similarity	87.8 \pm 0.8	87.3 \pm 0.8	85.6 \pm 1.0	84.9 \pm 1.1	86.3 \pm 0.9	85.7 \pm 1.0
Learned Mean-Bound (sample)	88.2 \pm 3.1	87.6 \pm 3.2	84.1 \pm 1.5	83.5 \pm 1.5	88.4 \pm 0.9	87.9 \pm 1.1
Learned Max-Bound (sample)	*91.7 \pm 1.9	*91.3 \pm 2.1	83.5 \pm 1.6	82.9 \pm 1.6	89.9 \pm 1.4	89.6 \pm 1.3

D GRAPH CONSTRUCTION STRATEGY AND STORAGE

1055 **Symmetrizing Attention Matrices.** Although attention coefficients are learned in a directed manner,
 1056 we transform the resulting attention matrix $\alpha = \text{Attn}(X) \in R^{L \times L}$ into an undirected weighted
 1057 graph. After statistical filtering, we follow a row-wise operation. Given the row i , for each non-zero
 1058 entry α_{ij} , we introduce an edge (i, j) with weight $w_{ij} = \alpha_{ij}$. To enforce symmetry, each edge
 1059 induces its inverse edge by adding the edge (j, i) with its corresponding weight. If subsequent rows
 1060 in α reveal dependencies already calculated, we compare their attention coefficient and redefine the
 1061 edge weight as

$$w_{ij} = w_{ji} = \max(\alpha_{ij}, \alpha_{ji}). \quad (10)$$

1063 This process ensures a consistent undirected representation while preserving the strongest dependencies
 1064 between sentence nodes.

1066 **Single-Pass Graph Construction.** The resulting learned document graphs are precomputed and
 1067 stored as PyTorch Geometric objects. Unlike alternative approaches constructing graphs on the fly,
 1068 our implementation incurs the graph-creation cost only once, significantly reducing computational
 1069 overhead by eliminating the need for graph reconstruction across epochs and model variations.

E GRAPH-BASED VS. NON-GRAPH APPROACHES

E.1 CLASSIFICATION METHODS

1076 While the focus of this work is on graph-based strategies for document representation and their
 1077 impact on document classification tasks, we also provide a comparative overview of recent non-
 1078 graph-based approaches utilizing traditional vector-based representations for document classifica-
 1079 tion. Table 6 summarizes the performance of recently proposed models on the datasets considered
 in this paper.

1080 Table 6: Classification results of our proposed learned graph structures compared to heuristic-based
 1081 graph construction methods and recent non-graph approaches. Reported metrics include accuracy
 1082 and macro-averaged F_1 score. Results marked with \ddagger are not directly comparable, as they use a
 1083 subsample of the arXiv dataset and only abstracts for classification.

1084

1085 1086 1087 1088 1089 1090 1091 1092 1093 1094 1095 1096 1097 1098 1099 1100 1101 1102 1103 1104 1105 1106 1107	1085 1086 1087 1088 1089 1090 1091 1092 1093 1094 1095 1096 1097 1098 1099 1100 1101 1102 1103 1104 1105 1106 1107		BBC News		HND		arXiv	
	Graph Scheme		Acc	F_1 -ma	Acc	F_1 -ma	Acc	F_1 -ma
<i>Non-graph-based strategies</i>								
Longformer-base		97.9	97.8	85.4	85.3	86.9	86.7	
LongT5-tglobal-base		96.3	96.3	74.6	74.5	87.8	87.8	
BERT (Park et al., 2022)		–	–	92.0	–	–	–	
CogLTX (Park et al., 2022)		–	–	94.8	–	–	–	
rRF (Singh et al., 2022)		96.2	96.1	–	–	–	–	
ConflBERT-SCR (Hu et al., 2022)		–	98.1	–	–	–	–	
Prefix-Propagation (Li et al., 2023a)		–	–	–	81.8	–	83.3	
LSG (Condevaux & Harispe, 2023)		–	–	–	–	–	87.9	
RAN+Random (Li et al., 2023b)		–	–	93.9	–	80.1	–	
RAN+GloVe (Li et al., 2023b)		–	–	95.4	–	83.4	–	
RAN+Pretrain (Li et al., 2023b)		–	–	96.9	–	85.9	–	
PFC (Yun et al., 2023)		98.1	97.1	–	–	\ddagger 76.0	\ddagger 61.0	
RoBERTa (Reusens et al., 2024)		98.0	97.0	–	–	–	–	
Llama-3.2-1B-Instruct (Li et al., 2025a)		–	–	–	–	89.2	89.0	
Llama-3.2-3B-Instruct (Li et al., 2025a)		–	–	–	–	90.4	90.3	
ModernBERT-base (Li et al., 2025a)		–	–	–	–	81.0	81.1	
AChorDS-LVQ (Mohammadi & Ghosh, 2025)		–	–	91.8	–	–	–	
<i>Heuristic-based graphs</i>								
complete graph		99.9	99.9	94.6	94.5	–	–	
sentence order		99.7	99.7	92.6	92.6	87.8	87.3	
window co-occurrence		99.8	99.8	92.1	92.1	87.9	87.4	
mean semantic similarity		99.4	99.3	91.2	91.1	–	–	
max semantic similarity		99.7	99.7	92.8	92.8	87.8	87.3	
<i>Our learned graphs</i>								
learned mean-bound		99.9	99.9	95.0	94.9	–	–	
learned max-bound		99.6	99.6	92.6	92.6	91.9	91.7	

1108

1109

1110 Park et al. (2022) fine-tuned several Transformer-based models, including **BERT** (Devlin et al.,
 1111 2018) and **CogLTX** (Ding et al., 2020). BERT was fine-tuned on truncated inputs to the first 512
 1112 tokens, using a fully connected layer on the [CLS] token for classification. In turn, the Cognize
 1113 Long TeXts (CogLTX) model was included in the study with the hypothesis that a small set of key
 1114 sentences is sufficient for accurate document classification.

1115

1116 Another method, **rRF** (removal of Redundant Feature) (Singh et al., 2022) applies dimensionality
 1117 reduction by eliminating redundant information based on word-level similarity scores computed
 1118 using GloVe embeddings (Pennington et al., 2014), followed by a Naive Bayes classifier.

1119

1120 **ConflBERT** (Hu et al., 2022) is a domain-specific pre-trained language model for conflict and po-
 1121 litical violence detection. Although the authors explore both pretraining from scratch and continual
 1122 pretraining strategies, Table 6 only reports the best-performing variant – pretrained from scratch
 1123 using cased data (SCR).

1124

1125 Although parameter-efficient tuning methods aim to reduce memory overhead while attaining com-
 1126 parable performance to fine-tuning of pretrained language models, they often fail to model long
 1127 documents. To address this, Li et al. (2023a) propose **Prefix-Propagation**, a technique that allows
 1128 prefix hidden states to dynamically evolve across layers by incorporating them into the attention
 1129 mechanism.

1130

1131 To further mitigate the quadratic complexity of Transformer self-attention for long sequences, Lo-
 1132 cal Sparse Global (**LSG**) attention is proposed in (Condevaux & Harispe, 2023). LSG follows a
 1133 block-based processing of the input and applies local attention to capture local context for nearby
 1134 dependencies, sparse attention for extended context, and global attention to improve information
 1135 flow inside the model.

1136

1137 In a similar direction, Li et al. (2023b) propose the Recurrent Attention Network (**RAN**), which
 1138 introduces a recurrent formulation of self-attention to handle long sequences, enabling long-

1134 term memory and extracting global semantics in both token-level and document-level representations.
 1135 RAN processes sequences in non-overlapping windows, applying positional multi-head self-
 1136 attention to a window area, and propagates a global perception cell vector across windows to capture
 1137 long-term dependencies. Table 6 presents results for three RAN variants: i) RAN+Random, with
 1138 randomly initialized weights; ii) RAN+GloVe, using GloVe embedding (Pennington et al., 2014) as
 1139 word representation; and iii) RAN+Pretrain, pretrained with a masked language modeling objective
 1140 on the BookCorpus (Zhu et al., 2015) and C4 (RealNews-like subset) (Raffel et al., 2020).

1141 To further reduce the computation of self-attention, Yun et al. (2023) propose a **PFC** strategy, which
 1142 integrates a token pruning step to eliminate less important tokens from attention computations, and
 1143 a token combining step to condense input sequences into smaller sizes.

1144 Despite such innovations, full model fine-tuning remains widely adopted in document classification.
 1145 For instance, a fine-tuned **RoBERTa** (Liu et al., 2019) was used by Reusens et al. (2024), combining
 1146 Bayesian search with author recommendations for hyperparameter setting. Similarly, Li et al.
 1147 (2025a) evaluate small language models in real-world classification tasks, focusing on best practices
 1148 and tuning strategies to address text classification effectively. The study included **Llama3.2 (1B-3B)**
 1149 (Touvron et al., 2023) and **ModernBERT-base** (Warner et al., 2024).

1150 Finally, Adaptive Chordal Distance and Subspace-based LVQ (**AChorDS-LVQ**) (Mohammadi &
 1151 Ghosh, 2025) is introduced as a prototype-based approach for learning on the manifold of linear
 1152 subspaces derived from input vectors. The method learns a set of subspace prototypes to represent
 1153 class characteristics and relevance factors, automating the selection of subspace dimensionalities
 1154 and the influence of each input vector on classification outcomes.

1156 E.2 CLASSIFICATION RESULTS

1158 In both the BBC News and arXiv datasets, our learned graph structures consistently outperform all
 1159 baseline models, including both heuristic-based graphs and recent non-graph approaches. On BBC
 1160 News, our learned mean-bound graphs achieve near-perfect performance with 99.9% accuracy and
 1161 F_1 score, significantly surpassing the best non-graph alternative, PFC, which reaches 98.1% accu-
 1162 racy and 97.1% F_1 score. Similarly, on arXiv, our learned max-bound graphs have a considerable
 1163 advantage over other graphs as well as over the strongest non-graph model, fine-tuned Llama-3.2.
 1164 While Llama-3.2 reports 90.4% accuracy for the 3B version and 89.2% accuracy for the 1B variant,
 1165 our learned graphs yield 91.9% accuracy and 91.7% F_1 score without requiring manual construc-
 1166 tions or task-specific expert knowledge. In contrast, on the HND dataset, heuristic-based graph
 1167 methods underperform compared to non-graph baselines. However, our learned graphs remain com-
 1168 petitive with top-performing models, such as RAN and CogLTX, demonstrating their capacity to
 1169 capture the document structure.

1170 The observed results underscore the effectiveness of automatically identifying task-relevant seg-
 1171 ments within input sequences, supporting the integration of local contextual information at lower
 1172 textual granularities while preserving global semantics at higher levels. Moreover, the performance
 1173 of RAN demonstrates the benefit of attention mechanisms that operate over windows with explicit
 1174 propagation of information from fine-grained units (e.g., tokens) to higher-level representations.
 1175 Such a strategy offers a clear advantage over conventional sequential models in constructing com-
 1176 prehensive document representations. The results from Table 6 further motivate future work to
 1177 explore alternative filtering strategies, other attention mechanisms, and hierarchical approaches to
 1178 constructing graphs over multiple text granularities (e.g., sentences, sections) via heterogeneous
 1179 graph structures.

1180 **Use of Large Language Models.** AI assistants were only used for paraphrasing and spell-
 1181 checking. All content, ideas, and claims presented in this paper remain the original work of the
 1182 authors.

1183
 1184
 1185
 1186
 1187